A Novel Hybrid Renewable Resources Constructed With Multilevel Inverter Using SVM Technique

Budi Srinivasarao, T Krishna Mohan, Swati Sharma, Devendra Nagal
Research Scholar Dept. of EEE Jodhpur National University, Asst.Prof Dept. of EEE ALIET, Vijayawada, Assoc.Prof., Asst.Prof, Dept. of EEE Jodhpur National University

Abstract-**The proposed system presents power-control strategies of a grid-connected hybrid generation system with versatile power transfer. This hybrid system allows maximum utilization of freely available renewable energy sources like wind, fuel and photovoltaic energies. For this, an adaptive MPPT algorithm along with standard perturbs and observes method will be used for the system. The objective of this paper is to study a novel Multi level multistring inverter topology for DERs based DC/AC conversion system. In this study, a high step-up converter is introduced as a front-end stage to improve the conversion efficiency of conventional boost converters and to stabilize the output DC voltage of various DERs such as PV, Wind and fuel cell modules for use with the simplified newly constructed multilevel inverter. The proposed multilevel inverter requires only nine active switches instead of the twelve required in the conventional cascaded H- bridge (CCHB) multilevel inverter, control with SVM technique. The inverter converts the DC output from non-conventional energy into useful AC power for the connected load. This hybrid system operates under normal conditions which include conventional and proposed cases of solar energy, fuel and wind energy. The proposed simulation results are presented to illustrate the operating principle, feasibility and reliability of this proposed system for Renewable resources.**

Index Terms—DC/AC power conversion, multilevel inverter.

I.INTRODUCTION

NOWADAYS, photovoltaic (PV) energy appears quite attractive for electricity generation because of its noiseless, pollution-free, scale flexibility, and little maintenance. Because of the PV power generation dependence on sun irradiation level, ambient temperature, and unpredictable shadows, a PV-based power system should be supplemented by other alternative energy sources to ensure a reliable power supply. Fuel cells (FCs) are emerging as a promising supplementary power sources due to their merits of cleanness, high efficiency, and high reliability. Because of long startup period and slow dynamic response weak points of FCs [1], mismatch power between the load and the FC must be managed by an energy storage system. Batteries are usually taken as storage mechanisms for smoothing output power, improving startup transitions and dynamic characteristics, and enhancing the peak power
capacity [2], [3]. Combining such energy sources introduces a PV/FC/battery hybrid power system. In comparison with single-sourced systems, the hybrid power systems have the potential to provide high quality, more reliable, and efficient power. In these systems with a storage element, the bidirectional power flow capability is a key feature at the storage port. Further input power sources should have the ability of supplying the load individually and simultaneously.

Many hybrid power systems with various power electronic converters have been proposed in the literature up to now. Traditional methods that integrate different power sources to form a hybrid power system can be classified into AC coupled systems [4], [5] and ac-coupled systems [6]–[12]. However, the main shortcomings of these traditional integrating methods are complex system topology, high count of devices, high power losses, expensive cost, and large size. In recent years, several power conversion stages used in traditional hybrid systems are replaced by multi-input converters (MICs), which combine different power sources in a single power structure. These converters have received more attention in the literature because of providing simple circuit topology, centralized control, bidirectional power flow for the storage element, high reliability, and low manufacturing cost and size. In general, the systematic approach of generating MICs is introduced in [13], in which the concept of the pulsating voltage source cells and the pulsating current source cells is proposed for deriving MICs. One of the samples of these MICs is utilized in [14] to hybridize PV and wind power sources in a unified structure. Besides, a systematic method to synthesize MICs is proposed in [15]. This paper deals with two types of MICs: in the first type, only one power source is allowed to transfer energy to the load at a time, and in the second type, all the input sources can deliver power to the load either individually or simultaneously. As another basic research in MICs, in [16] assumptions, restrictions, and conditions used in analyzing MICs are described, and then it lists some basic rules that allow determining feasible and un-feasible input cells that realize MICs from their single-input versions. Two multiple-input converters based on flux additivity in a multi winding transformer are reported in [17] and [18]. Because there was no possibility of bidirectional operating of the converter in [17], and complexity of driving circuits and output power limitation in [18], they are not suitable for hybrid systems. In [19], a three port bidirectional converter with three active full bridges, two series resonant tanks, and a three- winding high-frequency transformer are proposed. In comparison with three-port circuits with only inductors and Diode Bridge at the load side, it gives higher boost gain and reduced switching losses due to soft-switching operation.

H. Tao et al. [20] present a family of multiport converters based on combination of dc link and magnetic

coupling by utilizing half-bridge boost converters. The system features minimum number of conversion steps, low cost, and compact packaging. In [21], the input–output feedback control linearization for a DC–AC bidirectional MIC composing a high frequency isolating link transformer, two half-bridge boost converters at the input ports and a bidirectional cycloconverter at the output port is proposed. In [12]-[14], three MICs are proposed based on structure of the dc–dc boost converter. The dc–dc boost converter in [12] is useful for combining several energy sources whose power capacity or voltage levels are different. The multi input dc–dc converter proposed in [13] has the capability of operating in different converter topologies (buck, boost, and buck–boost) in addition to its bidirectional operation and positive output voltage without any additional transformer. A three input dc–dc boost converter proposed by authors in [14] can combine a Wind, PV, an FC, and a battery in a simple unified structure. A comprehensive power management algorithm is realized in order to achieve maximum power point tracking (MPPT) of the PV source and set the FC in its optimal power operation range. A three port isolated full bridge topology is proposed in [3] for hybrid FC/battery system, which its aim is feeding a small autonomous load. This topology gains the advantage of bidirectional power flow due to the active full bridges in each port. Based on the model of the transformer reported in [3], the three transformer coupled half bridge converters proposed in [25] are analyzed. Thereby, phase-shift control method is used to manage the power flow among the three ports in addition to soft switching for all switches over a wide input range.

Wai et al. presents two kinds of MICs in [2] and [16]. a high step-up ratio bidirectional MIC with high efficiency is proposed. The converter operates in standalone state, united power supply state, and charge and discharge states. A two input power converter for a hybrid FC/battery power system is proposed in [2] with zero voltage switching characteristic. Although the circuit efficiency is greatly developed, the converter does not provide bidirectional functionality and is not able to boost the input voltage to a higher level. Moreover, the summation of duty ratios should be greater than 1 and the two input voltages should be in the same level in the dual power supply operation state. Qian et al. presents a hybrid power system consist of a PV and a battery for satellite applications, and a four port hybrid power system supplied by a PV, a wind, and a battery ,a power control strategy is designed to manage the charge balance of the battery in order to regulate the output voltage. In these systems, the PV and the wind sources are exploited in MPPT conditions. Moreover, control strategies of the both systems are designed based on small signal modeling of the converters. Proper decoupling method is productively introduced to separately design compensators for cross coupled control loops.

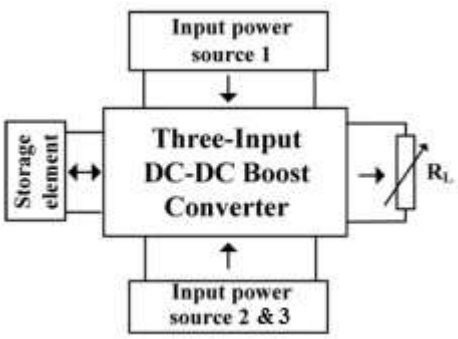

Fig.1 Proposed system overview.

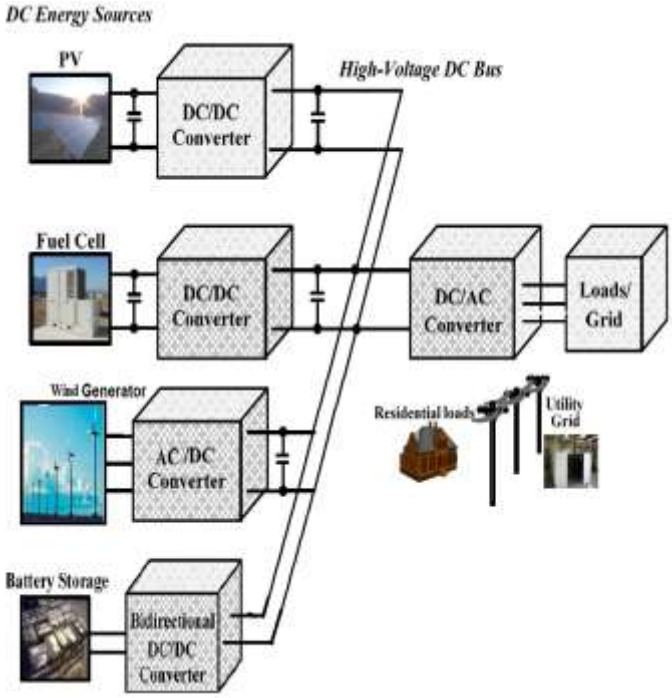

Fig.2 Configuration of multi string inverter for various DERs application.

In this paper, a new four input dc–dc boost converter is proposed for hybrid power system applications. As shown in Fig. 1, the proposed converter interfaces three unidirectional ports for input power sources, a bidirectional port for a storage element, and a port for output load in a unified structure. The converter is current source type at the both input power ports and is able to step up the input voltages. The proposed structure utilizes only four power switches that are independently controlled with four different duty ratios. Utilizing these duty ratios facilitates controlling the power flow among the input sources and the load. Powers from the input power sources can be delivered to the load individually or simultaneously.

2. POWER CONTROL TECHNIQUES FOR CONVERTER STAGES:

A. High Power Converter Stage:

In this study, high Power converter topology in [26] is introduced to boost and stabilize the output DC voltage of various DERs such as PV, Wind and fuel cell modules for employment of the proposed simplified multilevel inverter. The architecture of a high power converter initially introduced from [26], depicted in Fig. 7, and is composed of different converter topologies: boost, fly back, and a charge pump circuit.

The coupled inductor of the high power converter in Fig. 7 can be modeled as an ideal transformer, a magnetizing

inductor, and a leakage inductor. According to the voltage seconds balance condition of the magnetizing inductor the voltage of the primary winding can be derived as

$$v_{pri} = v_{in} \cdot {}^{D}/_{(1-D)} \quad (1)$$

Where V_{in} represents each the low-voltage DC energy input sources, and voltage of the secondary winding is

$$v_{sec} = {}^{N_S}/_{N_p} \cdot v_{pri} = {}^{N_S}/_{N_p} \cdot V_{in} \cdot {}^{D}/_{(1-D)} \quad (2)$$

Similar to that of the boost converter, the voltage of the charge-pump capacitor C_{pump} and clamp capacitor Cc can be expressed as

$$v_{cp} = v_{Cc} = V_{in} \cdot {}^{1}/_{(1-D)} \quad (3)$$

Hence, the voltage conversion ratio of the high step-up converter, named input voltage to bus voltage ratio, can be derived as [26]

$$\frac{V_{si}}{V_{in}} = \left(2 + \frac{N_s}{N_p} \cdot {}^{D}/_{(1-D)}\right)\Big|_{i=1,2} \quad (4)$$

B. Simplified Multilevel Inverter Stage:

To assist in solving problems caused by cumbersome power stages and complex control circuits for conventional multilevel inverters, this work reports a new three-phase multi string topology, presented as a new basic circuitry in Fig. 3.

Referring to Fig. 7, it should be assumed that, in this configuration the three capacitors in the capacitive voltage divider are connected directly across the DC bus, and all switching combinations are activated in an output cycle. The dynamic voltage balance between the two capacitors is automatically controlled by the preceding high step-up converter stage. Then, we can assume $Vs_1=Vs_2=Vs3=Vs$.

This topology includes nine power switches—three fewer than the CCHB inverter with twelve power switches - which drastically reduces the power circuit complexity and simplifies modulator circuit design and implementation. The PD PWM control scheme is introduced to generate switching signals and to produce five output-voltage levels: zero, V_S, $2V_S$, $-V_S$, and $-2V_S$.

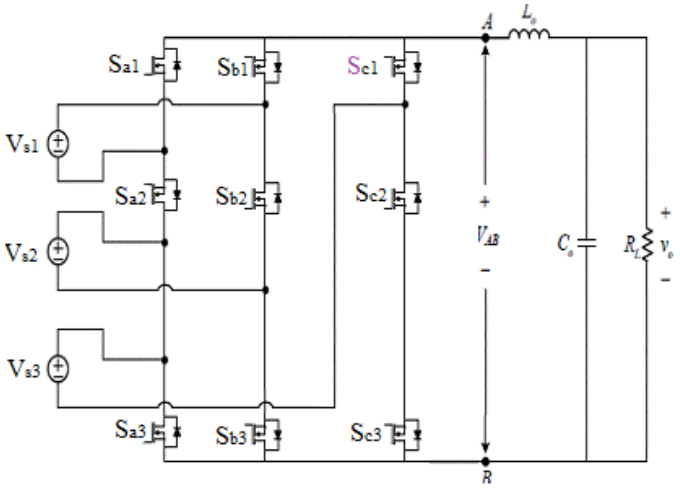

Fig.3. Basic Seven-level inverter circuitry.

This inverter topology uses two carrier signals and one reference to generate PWM signals for the switches. The modulation strategy and its implemented logic scheme in Fig.4 is a widely used alternative for phase disposition modulation. With the exception of an offset value equivalent to the carrier signal amplitude, two comparators are used in this scheme with identical carrier signals V_{tri1} and V_{tri2} to provide high-frequency switching signals for switches S_{a1}, S_{b1}, S_{a3} and S_{b3}. Another comparator is used for zero crossing detection to provide line-frequency switching signals for switches Sa2 and Sb2.

For convenient illustration, the switching function of the switch in Fig. 3 is defined as follows

$$S_{aj} = \begin{cases} 1, & S_{aj} \text{ ON} \\ 0, & S_{aj} \text{ OFF} \end{cases} \quad ,j=1, 2, 3 \quad (5)$$

$$S_{bj} = \begin{cases} 1, & S_{bj} \text{ ON} \\ 0, & S_{bj} \text{ OFF} \end{cases} \quad ,j = 1,2,3 \quad (6)$$

$$S_{cj} = \begin{cases} 1, & S_{cj} \text{ ON} \\ 0, & S_{cj} \text{ OFF} \end{cases} \quad ,j = 1,2,3 \quad (7)$$

Table I. lists switching combinations that generate the required seven output levels. The corresponding operation modes of the multilevel inverter stage are described clearly as follows.

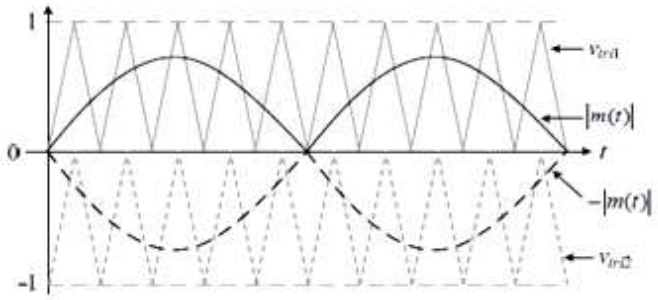

Fig.4 Modulation strategy: carrier/reference signals

Table-1

Switching Combinations

S_{a1}	S_{a2}	S_{a3}	S_{b1}	S_{b2}	S_{b3}	Sc1	Sc2	Sc3	V_{AB}
0	1	0	1	0	1	0	0	1	$2v_s$
0	1	1	1	0	0	0	1	1	v_s
1	1	0	0	0	1	1	1	1	v_s
1	1	1	0	0	0	0	0	0	0
0	0	0	1	1	1	1	0	0	0
1	0	0	0	1	1	0	0	1	$-v_s$
0	0	1	1	1	0	1	0	1	$-v_s$
1	0	1	0	1	0	1	1	0	$-2v_s$

To verify the feasibility of the three-phase seven-level inverter, a widely used software program PSIM is applied to simulate the circuit according to the previously mentioned

operation principle. The control signal block is shown in Fig. 4. m(t) is the sinusoidal modulation signal. Both V_{tri1} and V_{tri2} are the two triangular carrier signals. The peak value and frequency of the sinusoidal modulation signal are given as m_{peak}=0.7 and f_m=60Hz, respectively. The peak-to-peak value of the triangular modulation signal is equal to 1, and the switching frequency f_{tri1} and f_{tri2} are both given as 1.8kHz.

The three input voltage sources feeding from the high step-up converter is controlled at 100V, i.e. $V_{s1}=V_{s2}=Vs3=100V$. The simulated waveform of the phase voltage with seven levels is shown in Fig. 5. The switch voltages of S_{a1}, S_{a2}, S_{a3}, S_{b1}, S_{b2}, S_{b3},S_{c1},S_{c2} and S_{c3} are all shown in Fig. 6.

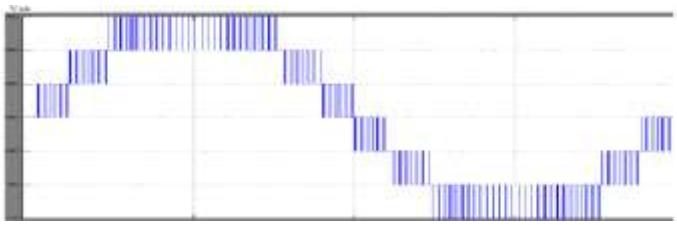

Fig.5 simulated waveforms pf phase voltage V_{AB} of inverter stage [Scale: 100V/div]

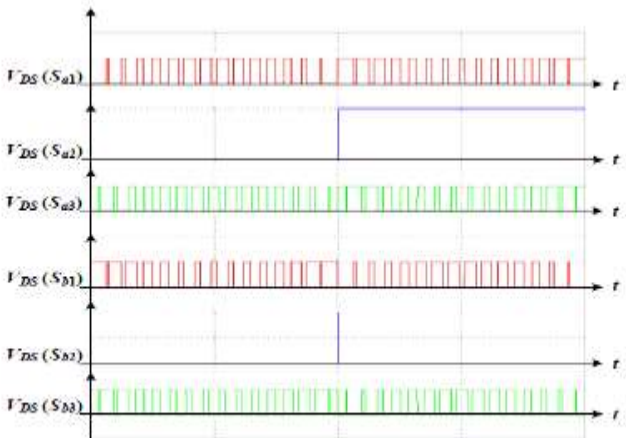

Fig.6. Simulated waveforms of switch voltage for inverter stage with in a line period [Scale: 100V/div]

The average switching power loss Ps in the switch caused by these transitions can be defined as

Ps □□0.5VDS I o f s □tc (on) □□tc (off) □ (8)

Where tc (on) and tc (off) are the turn-on and turn-off crossover intervals, respectively; V_{DS} is the voltage across the switch; and Io is the entire current which flows through the switch. The voltage stresses of the nine switches of the CCHB inverter are all equal to V_s.

For simplification, both the proposed circuit and CCHB inverter are operated at the same turn-on and turn-off crossover intervals and at the same load Io. Then, the average switching power loss P_s is proportional to V_{DS} and f_s as

$$P_s \alpha V_{DS}.f_s \quad (9)$$

According to Eq. (9) the switching losses of the CCHB inverter from twelve switches can be, obtained as

$$P_{s,\ H\text{-}bridge} \alpha 8V_s f_s \quad (10)$$

Similarly, the switching power loss of the proposed three phase seven-level inverter due to nine switches can also be obtained as

$$P_{s,\ proposed} \alpha 4Vsfs+2(2V_s)\ f_m \alpha 4V_s\ (f_s+f_m). \quad (11)$$

Because switches S_{a2}, S_{b2} can only be activated twice in a line period (60Hz) and the switching frequency is larger than the line frequency ($f_s>>f_m$), the switching losses of the proposed circuit is approximated to $4V_sf_s$. obviously, the switching power loss is nearly half that of the CCHB inverter.

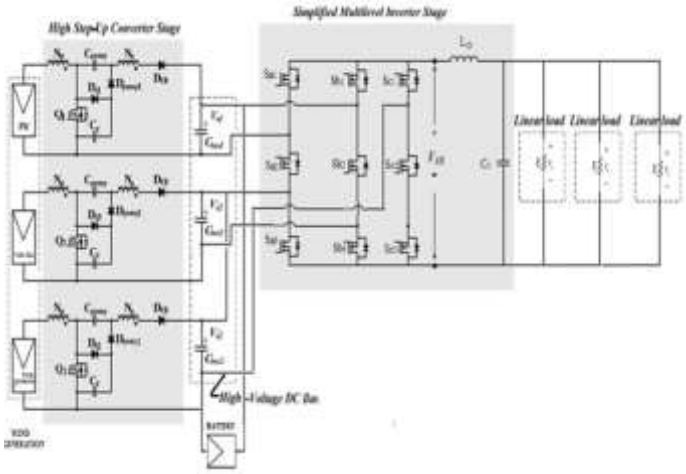

Fig.7.Multi-levelinverter topologies of CCHB inverter [15]

Considering the harmonics in the inverter output voltage V_{AB}, the amplitude of the fundamental and harmonic components in the output voltage V_{AB} are calculated by MATLAB software. The phase shift SVM technique is adopted for the CCHB Inverter. the CCHB multilevel inverter is operated in the same condition, including the same switching frequency 18kHz and modulation index ,the same input voltage VS=100V and output L-C filter, Lo=1mH, Co=4.7uF.

C. DC-AC Power converter space vector modulation Technique.

Nine power switches of inverter with 8 possible combinations shown in "Figure. 7" are corresponding to effective voltage space vector U1 – U_9 and 2 zero vector U_0,U_9. The phase angle between one effective voltage space vector and adjacent one is 40 degrees. They constitute 9 uniform segments. The three digits in brackets express the linking state between three-phase output A,B,C and the input DC, such as M=101 which represents the switching of the switches S_{ai},S_{bj} and S_{ck}

The output voltage space vectors and the corresponding switching states are represented in "Fig. 8".

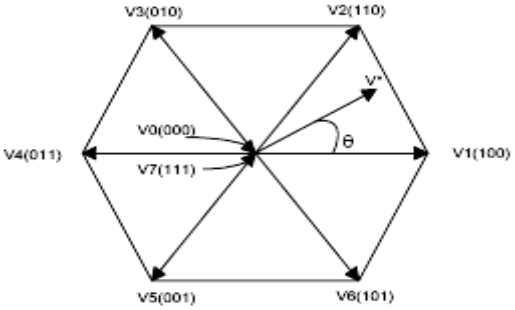

Fig.8,The composition of output voltage vector and Switching stages.

Any expected output voltage space vector U_J is formed by adjacent two basic output voltage vectors U_M, U_N,Uz t and zero output voltage U_0 orU9. Suppose the angle between U_J and U_M is θ_J .

$$U_J = d_M U_M + d_N U_N + d_0 U_0 \quad (12)$$

Whered_M, d_N and d_0 are the ratio cycles of U_M, U_N and U_0 respectively. And

$$d_M = T_M / T_\delta = m_v \sin(60^0 - \theta_J) \quad (13)$$

$$d_N = T_N / T_\delta = m_v \sin(\theta_J) \quad (14)$$

$$d_0 = 1 - d_M - d_N \quad (15)$$

Where T_M, T_N is the switching time of vectors U_M and U_N respectively. T_δ is the switching period of PWM. m_v is the modulation index of output voltage. And

$$m_v = (2/3)^{1/2} U_{om} / (U_{im} m_c \cos \emptyset) \quad (16)$$

Where U_{om} and U_{im} are the amplitude of output and input voltage, m_c is the input current modulation index, generally set $m_c = 1$, $\emptyset$ is the input power factor angle. When the rotating space vector U_J locates in a segment, the local average of output voltage can be formed by two adjacent basic voltage space vectors constituting this segment and one zero voltage space vector.

D. SVM Techniques

A different approach to SPWM is based on the space vector representation of voltages in the d, q plane. The d, q components are found by Park transform, where the total power, as well as the impedance, remains unchanged.Fig:9 space vector shows space vectors in according to 9 switching positions of inverter, V* is the phase-to-center voltage which is obtained by proper selection of adjacent vectors V1 and V2.

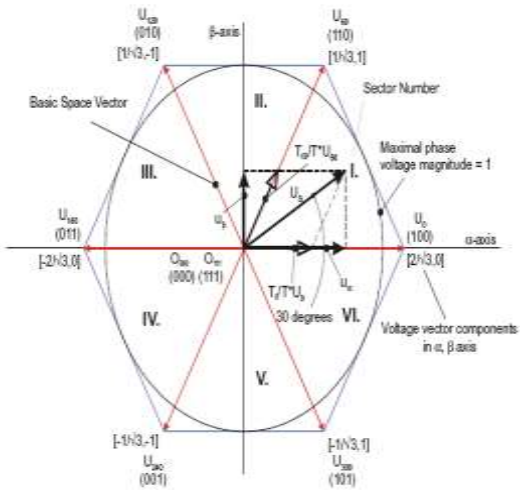

Fig.9. Inverter output voltage space vector

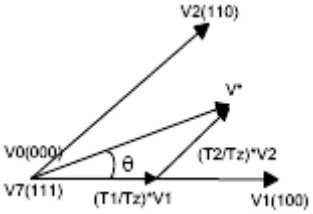

Fig 9.1 Determination of Switching times

The reference space vector V* is given by Equation (17), where T1, T2 are the intervals of application of vector V1 and V2 respectively, and zero vectors V0 and V7 are selected for T0.

V* Tz = V1 *T1 + V2 *T2 + V0 *(T0/2) + V7 *(T0/2)…….(17)

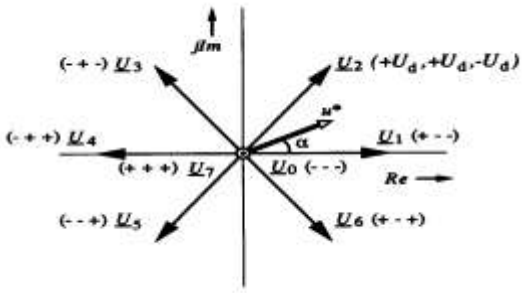

Fig 9.2 Space vector Modulation

The amplitude of u0 and u9 equals 0. The other vectors u1…u9 have the same amplitude and are 40 degrees shifted. By varying the relative on-switching time T_{on} of the different vectors, the space vector u* and also the output voltages ua, ub and uc can be varied and is defined as:

ua = Re (u*)

ub = Re (u* . a-1)

uc = Re (u* . a-2) ……(18)

During a switching period Ton and considering for example the first sector, the vectors u0, u1 and u2 will be switched on alternatively.

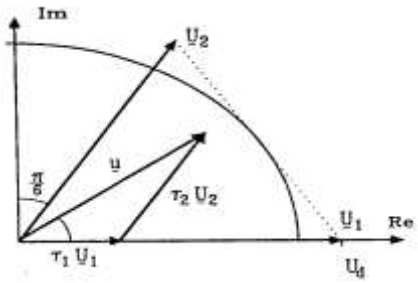

Fig.9.3 Definition of the Space vector

Depending on the switching times t0, t1 and t2 the space vector u* is defined as:

u* = 1/Ton . (t0. u0 + t1. u1 + t2. u2)

u* = t0 . u0 + t1. u1 + t2. u2

u* = t1 . u1 + t2. u2 …….. (19)

Where

t0 + t1 + t2 = Ton and

t0 + t1 + t2 = 1

t0, t1 and t2 are the relative values of the on witching times. They are defined as: t1 = m. cos (a + p/6),

t2 = m. sin a t0 = 1 - t1 - t2

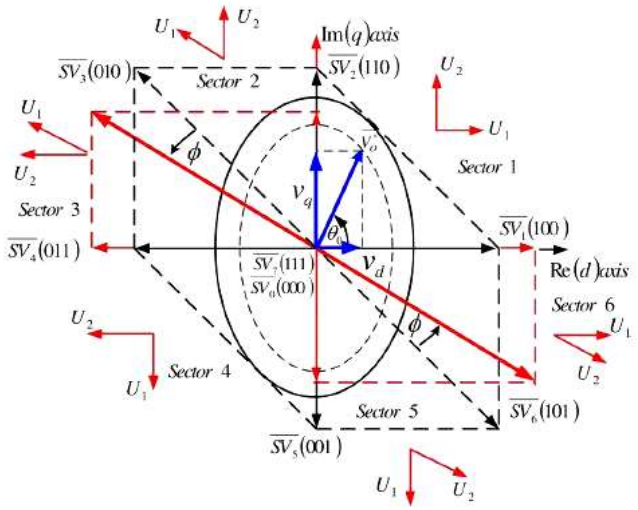

Fig 9.4. SVM Vector Diagram for New Switching Converter

Their values are implemented in a table for a modulation factor m = 1. Then it will be easy to calculate the space vector u* and the output voltages ua, ub and uc. The voltage vector u* can be provided directly by the optimal vector control laws w1, v_{sa} and v_{sb}. In order to generate the phase voltages ua, ub and uc corresponding to the desired voltage vector u* the above SVM strategy is proposed.

Simulation Results:

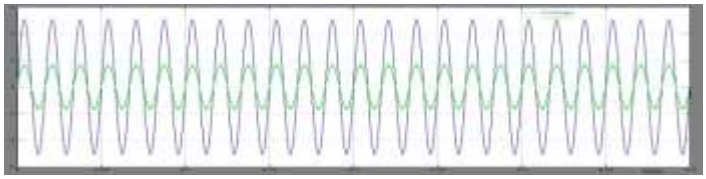

Fig.10.Output Voltage and Current with Unity Power factor

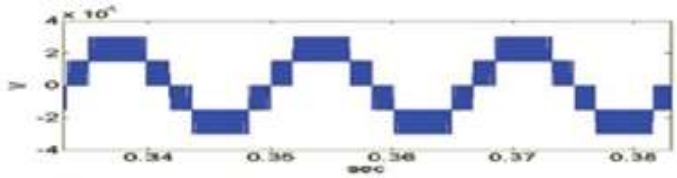

Fig.11 Inverter Output Five Level Voltage

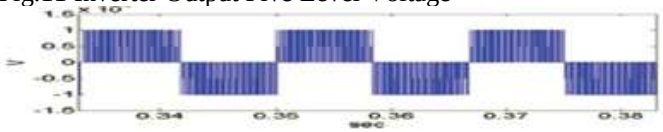

Fig.12 Inverter line voltage

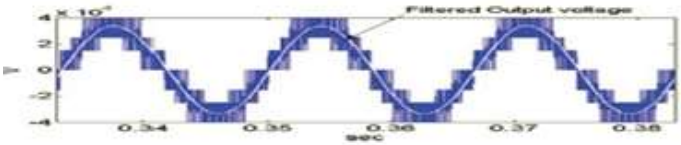

Fig.13 Inverter Output Seven Level Voltage

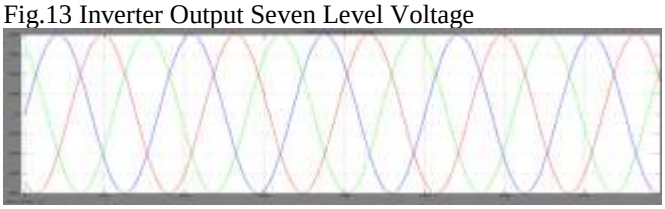

Fig.14 Load voltage with LC filters

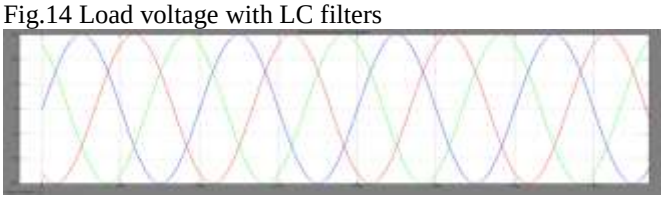

Fig.15Load Current with Lc filters wave forms

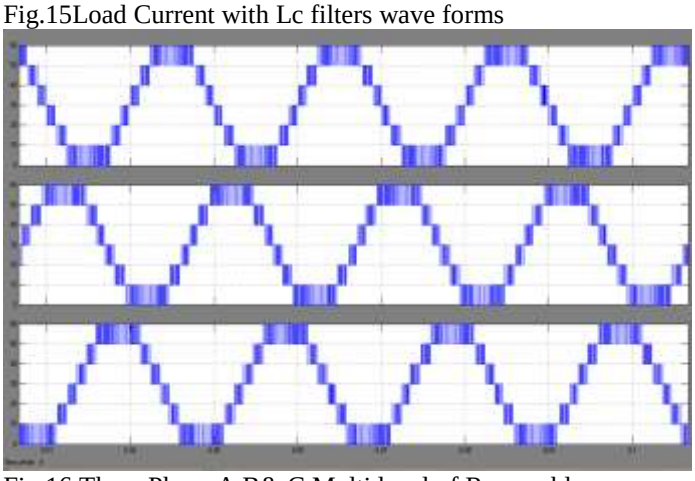

Fig.16 Three Phase A,B& C Multi level of Renewable power Inverter wave forms

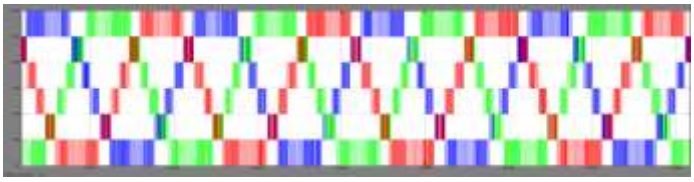

Fig.17 Three Phase Multi level of Renewable power Inverter Voltage with PLL Block Wave Forms

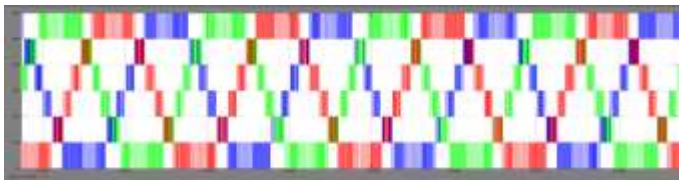

Fig.18 Three Phase Multi level of Renewable power Inverter Current with PLL Block Wave Forms

Table II
Components Parameters of the Proto Type

High Step DC/DC Converter Stage		
Components	Symbol	Value/Part no.
Coupling inductor	Lm, NP:NS	24µH, ETD 39,NP:NS = 1.5
Power switches	Q_1, $Q_{2,\ Q3}$	FDB3632,(100V, 9mΩ)
Charge-pump diodes	D_{pump1}, $D_{pump2,}$ D_{pump3}	STPS10AH100,(100V, 10A)
Clamping diodes	Dc1, Dc2, Dc3	STPS10AH100,(100V, 10A)
Output diodes	D_{O1}, D_{O2}	15ETH06S,(600V, 12A)
Charge-pump caps	$C_{\ pump}$	2×4.7µF/630V
Bus capacitors	C_{bus1}, $C_{bus2,}$ C_{bus3}	2000uF/400V
Simplified Multilevel DC/AC stage		
Power switches	S_{a1}, S_{a2}, $S_{a3,}$ S_{b1}, S_{b2}, S_{b3} Sc1,sc2,sc3	FDB2710,(250V, 2.5mΩ
Output inductor	L_o	1mH
Output capacitor	C_o	4.7µF/630V

IV. CONCLUSIONS:

The proposed system illustrates Renewable & Sustainable power generation strategies of a grid system with versatile power transfer. This grid system allows maximum utilization of freely available renewable energy sources like fuel cell, WTG and photovoltaic energies. For this, an adaptive MPPT algorithm along with standard perturbs and observes (P&O) method will be used for the Wind, PV & Fuel system with DC/AC Power Converter with SVM Technique.

Also, this configuration allows the sources to supply the load separately or simultaneously depending on the availability of the energy sources. The turbine rotor speed is the main determinant of mechanical output from wind turbine to Permanent Magnet Synchronous Generator (PMSG) is coupled for attaining energy conversion system. Renewable energy resources like Fuel cell and Solar cell power generated are interconnected to DC Link.

The inverter converts the DC output from non-conventional energy into useful AC power for the connected load (Industrial & Commercial Loads). This Grid system operates under normal conditions which include normal room temperature or At Any atmospheric Condition.

This work reports a newly-constructed three-phase multi string multilevel inverter topology that produces a significant reduction in the number of power devices required to implement multilevel output for DERs. The studied inverter topology with SVM Technique offer strong advantages such as improved output waveforms, smaller filter size, and lower EMI. Total harmonic distortion (THD) of the voltage and current at the output of the Conventional inverter THD =1.45 and Proposed CCHB multi-level inverter THD= 0.54. Simulation results show the effectiveness of the proposed solution.

The Proposed simulation results are analyzed to illustrate the operating principle, feasibility and reliability of this proposed grid systems.

REFERENCES

[1] Y. Li, D. M. Vilathgamuwa, and P. C. Loh, “Design, analysis, and real-time testing of a controller for multi bus microgrid system,” IEEE Trans. Power Electronics, vol. 19, no. 5, pp. 1195-1204, Sept. 2004.

[2] N. Hatziargyriou, H. Asano, R. Iravani, and C. Marnay, “Micro grids,” IEEE Power and Energy Magazine, vol. 5, no. 4, pp. 78-94, Jul./Aug. 2007.

[3] F. Katiraei, R. Iravani, N. Hatziargyriou, and A. Dimeas, “Microgrids management,” IEEE Power and Energy Magazine, vol. 6, no. 3, pp. 54-65, May/Jun., 2008.

[4] C. L. Chen, Y. Wang, J. S. Lai, Y. S. Lee, and D. Martin, “Design of parallel inverters for smooth mode transfer microgrid applications,” IEEE Trans. Power Electronics, vol. 25, no. 1, pp. 6-15, Jan. 2010.

[5] C. T. Pan, C. M. Lai, and M. C. Cheng, “A novel high step-up ratio inverter for distributed energy resources (DERs),” IEEE International Power Electronics Conference-ECCE Asia, pp.1433-1437, 2010.

[6] C. T. Pan, C. M. Lai, and M. C. Cheng “A novel integrated single-phase inverter with an auxiliary step-up circuit for low-voltage alternative energy source application,” IEEE Trans. Power Electronics, vol. 25, no. 9, pp. 2234-2241, Sep. 2010.

[7] F. Blaabjerg, Z. Chen, and S. B. Kjaer, “Power electronics as efficient interface in dispersed power generation systems,” IEEE Trans. Power Electronics, vol. 19, no. 5, pp. 1184-1194, Sep. 2004.

[8] D. G. Infield, P. Onions, A. D. Simmons, and G. A. Smith, “Power quality from multiple grid-connected single-phase inverters,” IEEE Trans. Power Delivery, vol. 19, no. 4, pp. 1983-1989, Oct. 2004.

[9] S. B. Kjaer, J. K. Pedersen, and F. Blaabjerg “A review of single-phase grid-connected inverters for photovoltaic modules,” IEEE Trans. Industry Applications, vol. 41, no. 5, pp. 1292-1306, Sep./Oct. 2005.

[10] O. Lopez, R.Teodorescu, and J. Doval-Gandoy, “Multilevel transformer less topologies for single-phase grid-connected converters” IEEE Industrial Electronics Conference, pp. 5191-5196, 2006.

[11] T. Kerekes, R. Teodorescu, and U. Borup, “Transformer less photovoltaic inverters connected to the grid,” IEEE Applied Power Electronics Conference, pp. 1733-1737, 2007.

[12] G. Ceglia, V. Guzman, C. Sanchez, F. Ibanez, J. Walter, and M. I. Gimenez, “A new simplified multilevel inverter topology for DC-AC conversion,” IEEE Trans. Power Electronics, vol. 21, no. 5, pp. 1311-1319, Sep. 2006

[13] N. A. Rahim and J. Selvaraj, “Multi string five-level inverter with novel PWM control scheme for PV application,” IEEE Trans. Power Electronics, vol. 57, no. 6, pp. 2111-2123, Jun. 2010

[14] C. T. Pan, W. C. Tu, and C. H. Chen, “A novel GZV-based multilevel single phase inverter,” Taiwan Power Electronics conference, pp. 1391-1396, Sep. 2010.

[15] W. Yu, J. S. Lai, H. Qian, C. Hutchens, J. Zhang, G. Lisi, A. Djabbari, G. Smith, and T. Hegarty, “High-efficiency inverter with H6-type configuration for photovoltaic non-isolated AC module applications,” IEEE Applied Power Electronics Conference and Exposition, pp. 1056-1061, 2010.

[16] S. Vazquez, J. I. Leon, J. M. Carrasco, L. G. Franquelo, E. Galvan, M. Reyes, J. A. Sanchez, and E. Dominguez, “Analysis of the power balance in the cells of a multilevel cascaded H-bridge converter,” IEEE Trans. Industrial Electronics, vol. 57, no. 7, pp. 2287-2296, Jul. 2010.

[17] S. Daher, J. Schmid, and F. L.M. Antunes, “Multilevel inverter topologies for stand-alone PV systems,” IEEE Trans. Industrial Electronics, vol. 55, no. 7, pp. 2703-2712, Jul. 2008.

[18] M. Meinhardt and G. Cramer, “Past, present and future of gridconnected photovoltaic and hybrid-power-systems,” IEEE-PES Summer Meeting, pp. 1283-1288, 2000.

[19] S. Kouro, J. Rebolledo, and J. Rodriguez, “Reduced switching frequency modulation algorithm for high-power multilevel inverters,” IEEE Trans. Industrial Electronics, vol. 54, no. 5, pp. 2894-2901, Oct. 2007.

[20] S. J. Park, F. S. Kang, M. H. Lee, and C. U. Kim, “A new single-phase five level PWM inverter employing a deadbeat control scheme,” IEEE Trans. Power Electronics, vol. 18, no. 18, pp. 831-843, May 2003.

[21] L. M. Tolbert and T. G. Habetler, “Novel multilevel inverter carrier based PWM method,” IEEE Trans. Industry Applications, vol. 35, no. 5, pp. 1098-1107, Sep/Oct. 1999.

[22] Y. Liu, H. Hong, and A. Q. Huang, “Real-time calculation of switching angles minimizing THD for multilevel inverters with step modulation,” IEEE Trans. Industrial Electronics, vol. 56, no. 2, pp. 285-293, Feb. 2009.

[23] N. S. Choi, J. G. Cho, and G. H. Cho, “A general circuit topology of multilevel inverter,” IEEE Power Electronics Specialists Conference, pp. 96-103, 1991.

[24] G. Carrara, S. Gardella, M. Marchesoni, R. Salutari, and G. Sciutto, “A new multilevel PWM method: A theoretical analysis,” IEEE Trans. Power Electronics, vol. 7, no. 3, pp. 497-505, Jul. 1992.

[25] R. Gonzalez, E. Gubia, J. Lopez, and L. Marroyo, “Transformer less single-phase multilevel-based photovoltaic inverter,” IEEE Trans. Industrial Electronics, vol. 55, no. 7, pp. 2694-2702, Jul. 2008.

[26] W. Yu, C. Hutchens, J. S. Lai, J. Zhang, G. Lisi, A. Djabbari, G. Smith, and T. Hegarty, “High Efficiency Converter with Charge Pump and Coupled Inductor for Wide Input Photovoltaic AC Module Applications,” IEEE Energy Conversion Congress and Exposition, pp. 3895-3900, 2009.